Progress in Oceanography 149 (2016) 134–144

Contents lists available at ScienceDirect

Progress in Oceanography

journal homepage: www.elsevier.com/locate/pocean

Spatial variability of surface-sediment porewater pH and related water-column characteristics in deep waters of the northern South China Sea

Changgao Shao [a,b,c], Yi Sui [d,a], Danling Tang [a,b,f,*], Louis Legendre [e,a]

[a] State Key Laboratory of Tropical Oceanography, South China Sea Institute of Oceanology, Chinese Academy of Sciences, Guangzhou 510301, China
[b] University of Chinese Academy of Sciences, Beijing 100049, China
[c] MLR Key Laboratory of Marine Mineral Resources, Guangzhou Marine Geological Survey, Guangzhou 510075, China
[d] Department of Oceanography, Dalhousie University, Halifax, Nova Scotia B3H 4R2, Canada
[e] Sorbonne Universités, UPMC Univ. Paris 06, CNRS, Laboratoire d'Océanographie de Villefranche (LOV), Observatoire Océanologique, 06230 Villefranche-sur-Mer, France
[f] Collaborative Innovation Center for 21st-Century Maritime Silk Road Studies, China

ARTICLE INFO

Article history:
Received 6 April 2016
Received in revised form 27 September 2016
Accepted 12 October 2016
Available online 1 November 2016

Index terms:
1051
3022
1635
4219
4512

Keywords:
Surface-sediment porewater pH
Organic carbon
$CaCO_3$
South China Sea
Deep waters
Sediment

ABSTRACT

This study analyzes the pH of surface-sediment porewater (i.e. 2–3 cm below the water-sediment interface), and concentrations of $CaCO_3$ and organic carbon (OC) in 1192 sediment cores from the northern South China Sea, in water depths ranging from 137 to 3702 m. This is the first study in the literature to analyze the large-scale spatial variability of deep-water surface-sediment pH over a large ocean basin. The data showed strong spatial variations in pH. The lowest pH values (<7.3) were observed south of Hainan Island, an area that is affected by summer upwelling and freshwater runoff from the Pearl and Red Rivers. Moderately low pH values (generally 7.3–7.5) occurred in two other areas: a submarine canyon, where sediments originated partly from the Pearl River and correspond to a paleo-delta front during the last glacial period; and southwest of Taiwan Island, where waters are affected by the northern branch of the Kuroshio intrusion current (KIC) and runoff from Taiwan rivers. The surface sediments with the highest pH (⩾7.5, and up to 8.3) were located in a fourth area, which corresponded to the western branch of the KIC where sediments have been intensively eroded by bottom currents. The pH of surface-sediment porewater was significantly linearly related to water depth, bottom-water temperature, and $CaCO_3$ concentration ($p < 0.05$ for the whole sampling area). This study shows that the pH of surface-sediment porewater can be sensitive to characteristics of the overlying water column, and suggests that it will respond to global warming as changes in surface-ocean temperature and pH progressively reach deeper waters.

1. Introduction

Atmospheric levels of carbon dioxide have increased from 280 ppm in 1750 (beginning of the industrial era) to approximately 400 ppm in 2014, and may reach 500–1000 ppm at the end of twenty-first century (Houghton et al., 2001). The oceans have taken up 48% of the anthropogenic CO_2 released into the atmosphere since 1750 (Sabine et al., 2004), which has led to a decrease in seawater pH of 0.1 pH unit since pre-industrial times (Caldeira and Wickett, 2003). Ocean acidification could modify the structure and dynamics of ocean ecosystems (Doney et al., 2009).

The mechanisms that determine the pH of surface-sediment porewater (denoted "porewater" below for simplicity) are quite complex, i.e. more than those that affect the pH of seawater. The former mechanisms are related to physical and chemical characteristics of bottom water, the nature of the solid components of sediments and the dissolution of $CaCO_3$, and they may generally be linked to redox reactions in the sediments (Jourabchi et al., 2005). Organic carbon (OC) redox processes are among the most important sources of $[H^+]$ in porewater (Hales and Emerson, 1996; Reimers et al., 1996; Jourabchi et al., 2005). Most of the OC is oxidized in the upper few centimeters of the sediment, primarily utilizing dissolved molecular oxygen (Emerson and Bender, 1981;

---

[*] Corresponding author at: State Key Laboratory of Tropical Oceanography, South China Sea Institute of Oceanology, Chinese Academy of Sciences, 164 West Xingang Road, Guangzhou 510301, China.

E-mail addresses: shaochanggao@126.com (C. Shao), yz966445@dal.ca (Y. Sui), lingzistdl@126.com (D. Tang), legendre@obs-vlfr.fr (L. Legendre).

http://dx.doi.org/10.1016/j.pocean.2016.10.006
0079-6611/© 2016 Elsevier Ltd. All rights reserved.

Reimers et al., 1996). The environment beneath the oxygen-containing sediment layer is anoxic, and anaerobic bacteria are abundant there. These bacteria primarily oxidize OC by reducing sulfate to sulfide, denitrification, Mn reduction, Fe reduction, and methanogenesis (Ben-Yaakov, 1973; Nealson, 1997; Jourabchi et al., 2005). The OC metabolism can also stimulate the dissolution of $CaCO_3$ in sediments (Emerson and Archer, 1990; Jahnke and Jahnke, 2004), which process can also buffer the pH (Jourabchi et al., 2005).

Models developed to simulate chemical processes in a simplified ocean and in the underlying sediments (Ben-Yaakov, 1973; Jourabchi et al., 2005; Chen et al., 2006) show that, in a small-scale sediment environment, pH can vary significantly over short vertical distances (mm to cm) due to intense redox processes in surface sediments (Jourabchi et al., 2005). Similarly, experimental results in the laboratory have shown that changes in porewater pH could range between ±1 and 2 pH units over millimeters to centimeters and be time-dependent (Zhu et al., 2006), and both laboratory experiments and model simulation have shown that a sharp drop in pH typically occurred 2 cm below the sediment-water interface (Cai et al., 1995; Jourabchi et al., 2005; Zhu et al., 2006).

One recent report (Yanagawa et al., 2013) showed that porewater pH strongly affected the structure and activity of the microbial community in sediments, consistent with the fact that the oxidative action of anaerobic and aerobic bacteria is highly sensitive to porewater pH (Blake et al., 1993; Nealson, 1997). In addition, the low pH of porewater may affect the dissolution of $CaCO_3$ (Dolgaleva et al., 2005). Hence understanding the factors that control the spatial distribution of porewater pH can contribute to better understand the factors that determine microbial communities and $CaCO_3$ preservation in sediments. It is already known that porewater pH vary both spatially and temporally (Wolaver et al., 1986; Reimers et al., 1996), and small-scale horizontal variability of sediment pH is relatively well understood (Zhu et al., 2006). However, the spatial variability of pH over large geographic scales, in relation with water-column and other environmental characteristics, is poorly documented in the natural environment (Table 1). This is especially true of deep-sea environments, i.e. thousands of meters below the sea surface. The objectives of the present study are: to describe the large-scale spatial variability of deep-water sediment porewater pH over a large ocean basin, here the northern South China Sea (SCS; >300,000 km^2); and to explore the relationships of deep-water sediment porewater pH with physical and chemical characteristics of the overlying water column. We focused our study on surface-sediment pH because, from a geological viewpoint, the water-sediment interface is the gateway to long-term OC burial, and changes in its characteristics may influence the early diagenetic processes and mass exchanges. The present study is the first in the oceanographic literature to analyze the horizontal distributions of deep-water surface-sediment porewater pH on a large geographic scale.

2. Materials and methods

2.1. Study area

The study area was located along the continental slope of northern SCS (Fig. 1). Water depths of the sampling stations ranged from 137 to 3702 m. The complex land and sea northern SCS system is characterized by tropical monsoons, with winds that blow from the southwest in summer and from the northeast in winter, and anticyclonic and cyclonic water circulation during these two seasons, respectively, with a few stable eddies. The monsoon accelerates water-mass exchanges, creates upwelling, and produces complex physical, chemical and ecological characteristics (Tang et al., 1998, 2004; Chen et al., 2006; Sun et al., 2012). To the north, the Pearl River, which is the third largest river in China, connects the SCS to the hundreds of millions people who live along its course. To the east, the SCS is connected to the North Pacific Ocean

Table 1
Measurements of sediment pH in various studies.

Location	Surface sampled (10^3 km^2)	No. cores	No. pH measurements	Depths of pH measurements in the cores (m)	Water depth (m)	Range of pH values	Sampling years	References
Long Island Sound, Eastern USA (40.8°N; 73.2°W)	$(1.5–2.25)\times10^{-11}$	3	–	0–0.12	0–35	6–8.2	2003–2004	Zhu et al. (2006)
Gulf of Mexico (27.7°N;91.3°W)	41	3	–	0–0.12	522–548	7.4–8.6	2006	Cai et al. (2006)
Eastern South Atlantic (12°S-2.7°N; 6.3°E-13.1°E)	1150	4	–	0.06	1251–2185	7.2–7.9	1998	Wenzhöfer et al. (2001)
Ceara Rise, South Atlantic (3–6°N; 41–46°W)	180	6	~300	0.1	3270–4685	–	1994	Hales and Emerson (1997)
Ontong-Java Plateau, Pacific Ocean (0°N; 159–164°E)	0.1	3	~80	0–0.1	2322–2966	–	1991	Hales and Emerson (1996)
California continental rise (34.83°N; 123°W)	1×10^{-8}	3	~200	0.08	4100	7.2–7.95	1991	Cai et al. (1995)
Western North Atlantic (34.3–40°N; 69.5–72°W)	130	4	~60	0–0.03	2159–5210	–	1989	Hales et al. (1994)
Equatorial Atlantic Ocean (2.0°N-5.0°S; 22.77–23.00°W)	73	3	–	0–0.03	3858–5075	–	1987	Archer et al. (1989)
Lake Anna, Virginia, USA (38.06°N; 77.83°W)	0.004	4	31	0–0.3	–	6–7	1983	Herlihy and Mills (1986)
Lake Erie, Stony Brook Harbor, Whitehall Bay, USA (38.9–41.7°N; 73.2–82.3°W)	105	3	–	0–0.2	0.05–18	6–8	1979	Fisher and Matisoff (1981)
Guatemala Basin, North Pacific (8–12°N; 96–98°W)	91	2	21	0–0.52	3500–3900	7.4–7.7	1978	Murray et al. (1980)
World Ocean (IODP-USIO: Leg 100–346)	361000	–	13744	0.05–1531.15	95.5–5980	0.07–12.5	1985–2013	IODP-USIO (2014)
Northern South China Sea (15.6–22.5°N; 109.5–120°E)	325	1153	1153	0.02–0.03	137–3702	6.9–8.3	2000–2011	Present study

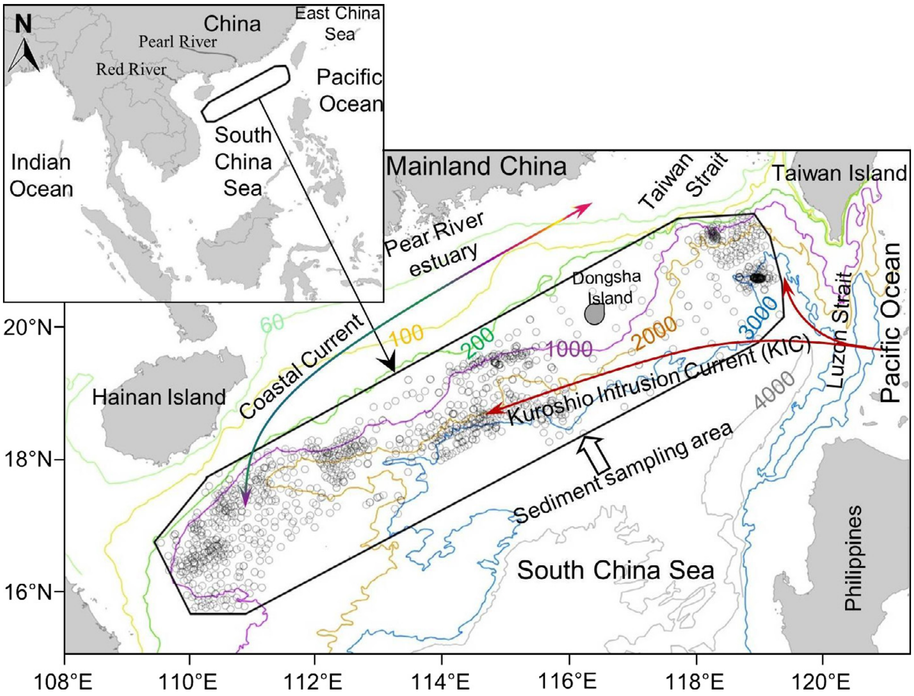

Fig. 1. Study area in the South China Sea showing the locations where the 1192 sediment cores were collected along the continental shelf.

and the East China Sea through the Luzon and Taiwan Straits, respectively, through which there are large exchanges of water. The seasonal water circulation in the eastern SCS is primarily driven by the monsoonal wind stress, and is greatly affected by the Kuroshio Intrusion Current (KIC) from the west Pacific Ocean (Gan et al., 2006). To the west, the area is bordered by lands on two sides, and typical continental-shelf upwelling usually occurs in summer (Tang et al., 2002; Jing et al., 2009).

The SCS basin has an elliptical shape. Its major axis is 2380 km long and oriented 30° to the NE, and the length of its approximately perpendicular minor axis is 150–450 km. Our study area (approximate surface area: 325,000 km^2) was located on the northern continental slope of that basin. This gentle slope had various geomorphical features that included seamounts, trenches, troughs, and submarine canyons (Liu et al., 2002).

2.2. Sampling and measurements

A total of 1192 sediment cores were collected between years 2000 and 2011, during 13 oceanographic cruises along the continental slope of the northern SCS. The cores were taken using a Benthos Piston Gravity Corer or a Benthos Gravity Corer, with a PVC plastic liner placed inside the steel core barrel. When the corer arrived on board the ship, the core in its plastic liner was extracted, and its surface section (upper 20 cm) was cut off quickly (within 5 min of core retrieval) and kept in its plastic liner. Measurements were only done on cores with good sediment-water interfaces, i.e. cores were not used when their surface section contained hard rocks, detritus, or the core surface was disturbed, because it did not offer proper material for inserting the pH sensor, or could have been invaded by seawater when the sediment core was collected.

The pH of the in-core sediment porewater was measured on the head end of the 20-cm surface section of the core using a Mettler Toledo FiveEasy™ pH Meter and Mettler Toledo pH Electrode LE438 sensor (resolution: ±0.01 pH unit; Mettler Toledo certified pH buffer solutions were used for pH sensor calibration; National Bureau of Standards, NBS, scale), without extraction from the plastic liner. The sensor was carefully inserted into the center of the head end of the sediment core section at a depth of 2–3 cm (i.e. the tip of the pH glass sensor reached the depth of 3 cm below the sediment surface; the diameter of the tip of the glass sensor was 0.4 cm), and the pH value was recorded as the sensor stabilized (i.e. within 0.5–1.0 min). This method was used to minimize the effect of temperature changes on the pH, and avoid exposure of the sediment sample to the air. In this study, every measurement was performed at least twice, and the mean value calculated. The pH measurement procedures were completed within 10 min of the core arrival on board the ship.

Temperature of all surface sediment sections was measured at the same time as pH using an instrument that combined a CENTER-300 thermocouple thermometer and TP-K02 immersion probe, for later temperature correction of the porewater pH. At the time of core sampling, the in situ bottom-water temperature above the seafloor was measured at some stations using a XXG-T Marine geothermal gradient measurement system (Luo et al., 2007), and seafloor depth was determined with a SeaBeam 2112 Multibeam Bathymetric Sonar (Fig. 2). After pH and temperature had been measured on board the ship, each 20-cm sediment-core section was sealed at both ends, and stored in a refrigerator at 4 °C. The OC and $CaCO_3$ concentrations were measured later in a land laboratory with the procedures of the Standardization Administration of the People's Republic of China (Yan and Huang, 1993; Zhang et al., 1998; Ma et al., 2008; Wang et al., 2010).

The pertinence of using the above methods for measuring porewater pH, including the type of glass electrode, is discussed in Section 4.1. The effects of changes in pressure and temperature during core recovery on pH measurements are also discussed in Section 4.1.

2.3. Data

The pH of porewater was measured on board the ship on 1153 of the 1192 cores taken in the northern SCS (Fig. 1), the in situ bottom-water temperature was measured at 91 stations (Fig. 2), and the concentrations of OC and $CaCO_3$ were determined on 549 of the 1192 cores. Because pH could not be measured on 36 of

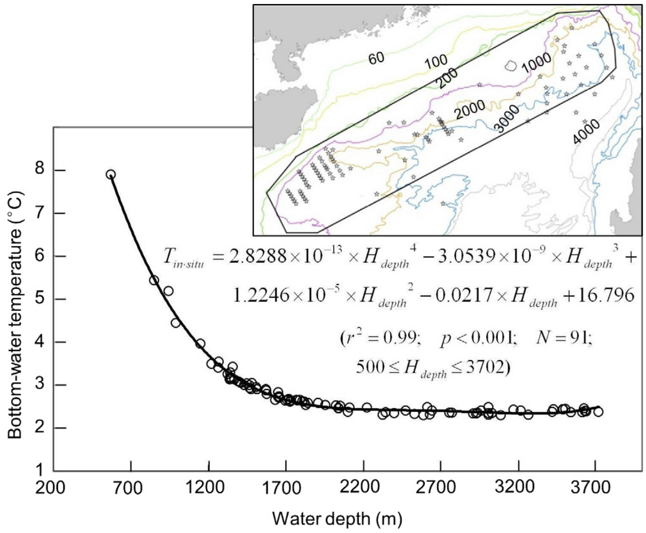

Fig. 2. Bottom-water temperature plotted as a function of water depth in northern SCS. The solid line corresponds to the polynomial regression given in the Figure, i.e. Eq. (2) in the text. Inset map: locations of the 92 stations where bottom-water temperature was measured.

these 549 cores (see above), the number of cores with measurements of the three variables (pH and the) was 513.

The porewater pH is sensitive to changes in temperature and pressure that occur when the core is transferred from its deep-sea environment to the ship. We corrected for temperature effects using the sediment temperature measured on board the ship (T_{ship}) (Gieskes, 1969; Ben-Yaakov, 1970):

$$pH_{temp\ corr} = pH_{ship} + 0.0093 \times (T_{ship} - T_{in\ situ}) \tag{1}$$

where $T_{in\ situ}$ is the in situ bottom-water temperature. We calculated the latter from water depth (H_{depth}) using the following regression equation that we derived from our 92 in situ bottom-water temperature measurements (Fig. 2):

$$\begin{aligned} T_{in\ situ} = {} & 2.8288 \times 10^{-13} \times H^4_{depth} - 3.0539 \times 10^{-9} \times H^3_{depth} + 1.2246 \\ & \times 10^{-5} \times H^2_{depth} - 0.0217 \times H_{depth} + 16.796 \end{aligned}$$

$$(r^2 = 0.99; \quad p < 0.0001; \quad N = 91; \quad 500 \leqslant H_{depth} \leqslant 3702) \tag{2}$$

The 0.0093 temperature coefficient in Eq. (1) was chosen based on the in situ characteristics of the deep-sea environment in our study area (temperature < 5 °C, salinity > 34, 6.9 < pH < 8.4; (Ben-Yaakov, 1970). Stations with water depths between 137 and 500 m were shallower than those where bottom temperature had been measured, but the bottom-water temperatures calculated with Eq. (2) corresponded well to measured temperatures at depths between 137 and 500 m in the water column of the SCS (Fig. 5 of Chou et al., 2007), i.e. differences were <1 °C, which would cause differences in pH < 0.01 according to Eq. (1). Hence we used Eq. (2) to compute bottom-water temperatures at all our sites including the 26 with water depths between 137 and 500 m.

We corrected for pressure effects using the hydrostatic pressure (P_{atm}) corresponding to the sampling depth:

$$pH_{in\ situ} = pH_{temp\ corr} - 0.000408 \times P_{atm} \tag{3}$$

where $P_{atm} = H_{depth}/10$. The constant value 0.000408 (pH·atm^{-1}) in Eq. (3) was calculated from the change in pH ($\Delta pH = 0.102$) that occurs when the pressure is changed from 0 to 250 atm ($\Delta P = 250$ atm) at temperature <5 °C, salinity = 34.8, and pH = 7.8 (Culberson and Pytkowicz, 1968), i.e. $\Delta pH/\Delta P = 0.000408$.

2.4. Data treatment

Spatially continuous pH values were obtained from the 1153 discrete data points using the natural neighbor interpolation method, which determines the weights of nearest points to be used to interpolate a new value. The method is based on Voronoi tessellation (Voronoi diagram), which divides the plane according to distance to points in various subsets of the plane (Franz, 1991). The basic equation is:

$$F(X, Y) = \sum_{i=1}^{n} W_i f(X_i, Y_i) \tag{4}$$

where $F(X, Y)$ is the interpolated value of the point at coordinate position (X, Y), W_i is a weight, and $f(X_i, Y_i)$ is the value of each data point (X_i, Y_i) around the (X, Y) point. The weights W_i are calculated based on the surrounding data when inserting (X, Y) into the tessellation (Sibson, 1981). We used the Arcmap software for the calculations, and for plotting contour lines to identify areas of low and high pH. We used the contour line pH = 7.5 to subdivide our study area into four regions.

We computed Model I linear regressions of porewater pH on water depth, bottom-water temperature, and percent concentrations of OC and $CaCO_3$. We performed *t*-tests to assess the statistical significance of the regression coefficients.

3. Results

3.1. Horizontal distribution of porewater pH

The 1153 pH measurements on porewater in the northern SCS ranged from 6.9 to 8.3 pH units (Fig. 3). Based on the horizontal distribution of the contour line pH = 7.5, we identified four broad regions (Fig. 4): south of Hainan Island (H), the Pearl River plume and the connected submarine canyon (P), the area influenced by the western branch of the KIC (K), and southwest of the coast of Taiwan Island (T). Region K had generally higher pH than the other regions (pH ⩾ 7.5 in most of the region, and up to 8.3 in its northern part); it corresponded to the western branch of the KIC along the northern continental slope. On the two sides of high-pH region K, the pH of porewater was generally lower. To the northeast of region K, region T (pH ⩽ 7.5 in most of the region) was affected by the northern branch of the KIC year-round, and by the influx of river water from the southwestern part of Taiwan Island. To the immediate southwest of region K, region P had moderately low pH (pH ⩽ 7.5 in most of the region); the northern part of that region was connected to the plume of the Pearl River, and most of its low porewater pH values were located in a submarine canyon (pH < 7.3). Further to the southwest, region H exhibited the lowest porewater pH of the northern SCS (pH < 7.3); it was characterized by upwelling in summer, and affected by freshwater from the Pearl and the Red Rivers carried by the coastal circulation. Overall, region K had the largest areas of surface sediments with pH ⩾ 7.5, and region H the largest areas with pH ⩽ 7.3.

3.2. Porewater pH, and water depth, bottom-water temperature, and OC and $CaCO_3$ concentrations

The linear regressions of porewater pH on environmental variables show that, for the whole sampling area, porewater pH was significantly related (p < 0.05) to water depth, bottom-water temperature and $CaCO_3$ concentration, but not OC concentration (Fig. 5). When considering each of the four regions, there were large scatters of data points in most bivariate plots that caused relatively low coefficients of determination, i.e. all r^2 were <0.18. Plots of residuals (Fig. 6) show that the points were most widely

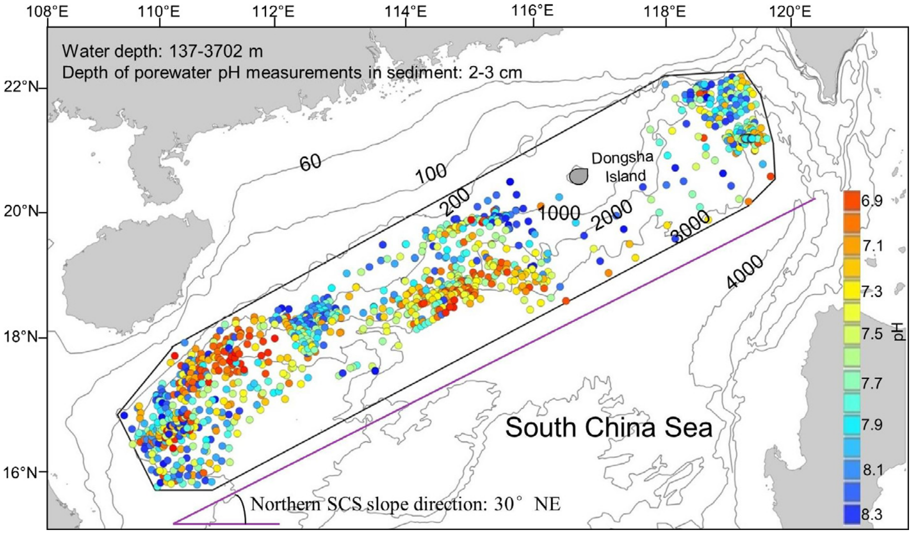

Fig. 3. Spatial distribution of the 1153 pH measurements, made 2–3 cm below the surface of the sediment cores.

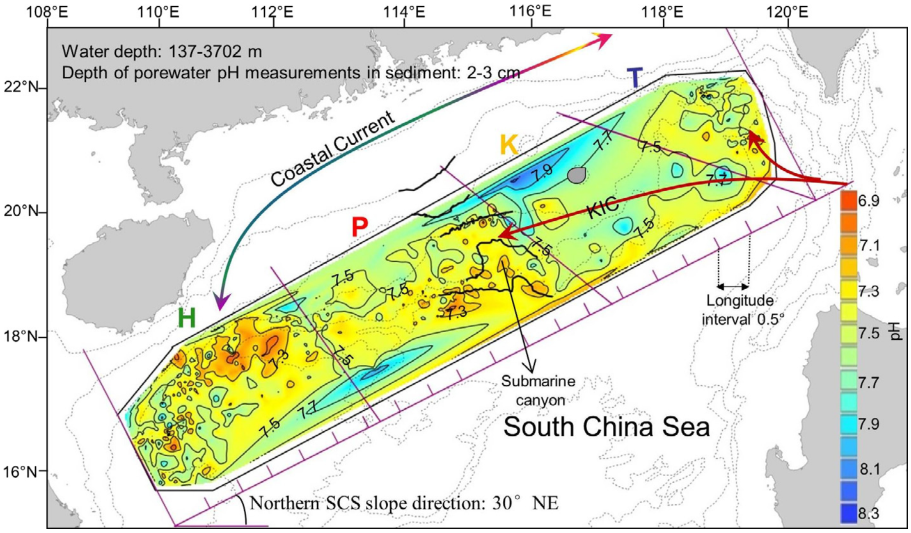

Fig. 4. Spatial distribution of pH (measured 2–3 cm below the surface of the sediment cores) resulting from the natural neighbor interpolation method using the discrete pH values measured on cores sampled at sites in Fig. 3, and contour lines pH = 7.3, 7.5, 7.7 and 7.9. The shape of the submarine canyon (black lines) was drawn based on the isobaths. Four regions were identified from the positions of the contour line pH = 7.5: H, P, K, and T (see text).

scattered relative to the regression line for water depth between 500 and 2000 m (500–2000 m in regions H and P, and 500–3500 m in region T), bottom-water temperature between 2 and 6 °C, $CaCO_3$ concentration <10 and >20%, and OC concentration between 0.6 and 1.2%. Deep-water sediments generally had low temperature and pH (Figs. 2 and 5a). Region T had the lowest surface-sediment $CaCO_3$ percent concentrations, whereas regions H and P had the highest, but the relationship between percent $CaCO_3$ and pH was different in these two regions, i.e. significantly positive in P and not significantly different from zero in H (Fig. 5c). Contrary to $CaCO_3$, surface-sediment OC percent concentrations tended to be quite similar in the four regions (Fig. 5d).

4. Discussion

4.1. Complementary approaches used to ensure the quality of pH measurements in porewater

The measurement of pH is sensitive to oxidation processes when the sediment is directly exposed to air, and when it experiences changes in temperature and pressure (Murray et al., 1980). In this study, we used the following approaches to ensure the quality of pH measurements on the sediment-core samples.

Firstly, it is known that redox processes are complex, and can change rapidly with depth below the sediment surface (Hales, 2003; Jourabchi et al., 2005). Laboratory experiments, model simulation and in situ pH measurements have indicated that the strongest vertical gradients in pH generally occurred in top 2 cm below the sediment-water interface (between 0.1 and 1.1 pH units cm^{-1} in Fig. 7), whereas vertical gradients were generally <0.15 pH unit cm^{-1} at the depth of 2–3 cm. Given that porewater pH is relatively constant between 2 and 3 cm below the sediment surface, this depth layer is suitable for porewater pH measurements, as was done in the present study.

Secondly, some sediment cores contained detritus in their top parts, and could thus have been invaded by seawater at the time of collection and retrieval. In such cases, the upper parts of the cores could have experienced strong diffusion of properties between the seawater and the porewater before the measurement of pH. To prevent this potential problem, the sediment cores with

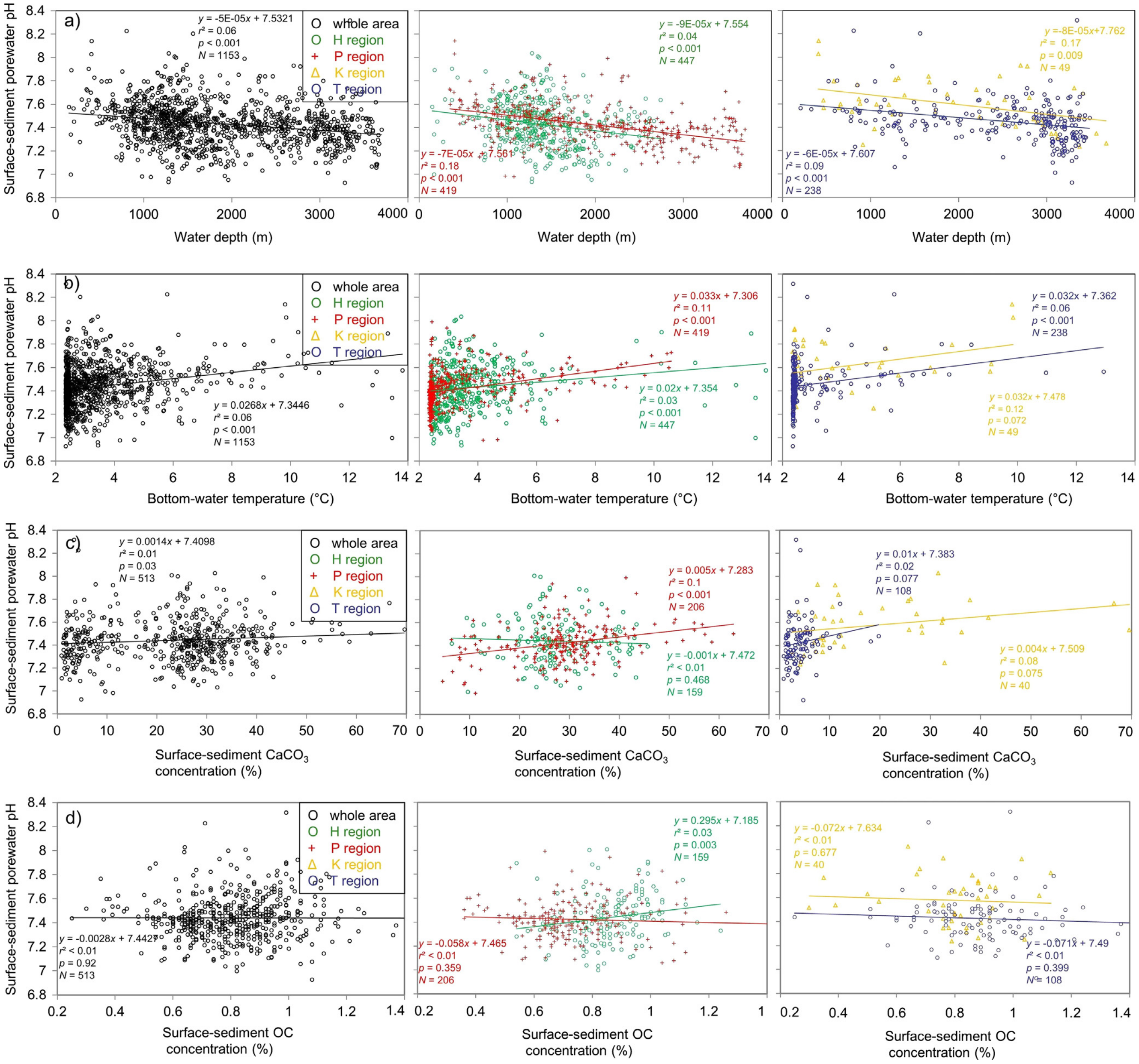

Fig. 5. Scatter diagrams and linear regressions of surface-sediment porewater pH versus (a) water depth, (b) bottom-water temperature, (c) surface-sediment $CaCO_3$ concentration, and (d) surface-sediment OC concentration in the whole sampling area and in the four regions identified in Fig. 4. Probability (p) that H_0: $b = 0$, where b is the regression coefficient.

detritus were not used. In addition, to avoid exposure of the samples to air and minimize the processing time of samples, these were not disturbed before measuring the pH, i.e. the pH was measured on the porewater within the cores as soon as these arrived on board the ship. This approach is different from that of IODP, where porewater pH is measured on extracted interstitial water (Expedition 302 Scientists, 2006; Expedition 329 Scientists, 2011), the cores are stored at low temperature (9 °C) and handled in an inert atmosphere when sampling the interstitial water, and the extraction of interstitial water to measure its pH may require from 1 to 50 h on board the ship. Our approach minimizes the time between the retrieval of the core and the measurement of pH.

Thirdly in order to minimize the temperature effects, the pH was measured on porewater directly inside the undisturbed core, without extraction, as soon as the core was retrieved on board the ship. Later, we corrected the measured pH for any difference between the in situ bottom-water temperature and that of the sediment core at the time of measurement, using Eqs. (1) and (2). For pressure changes, we corrected our pH data to the in situ hydrostatic pressure using Eq. (3). A similar method was also used by Culberson and Pytkowicz (1968) and Murray et al. (1980) to correct the pH in cases of differences between measurement and in situ temperature and pressure. Using our method, the accuracy of the correction will not be better than about ±0.02 pH units when the measurement and in situ temperatures differ by 20 °C (Gieskes, 1969). This is not as good as the temperature correction method of Hunter (Hunter, 1998) for the total, free and seawater pH scales, which reduces the error in the calculated pH to <0.0002 pH unit over the temperature range 0–40 °C. This correction is implemented in the R package 'seacarb' (Gattuso et al., 2014).

For our pH measurements, we used a commercial combined glass electrode (diameter: 0.4 cm), which immerses the reference

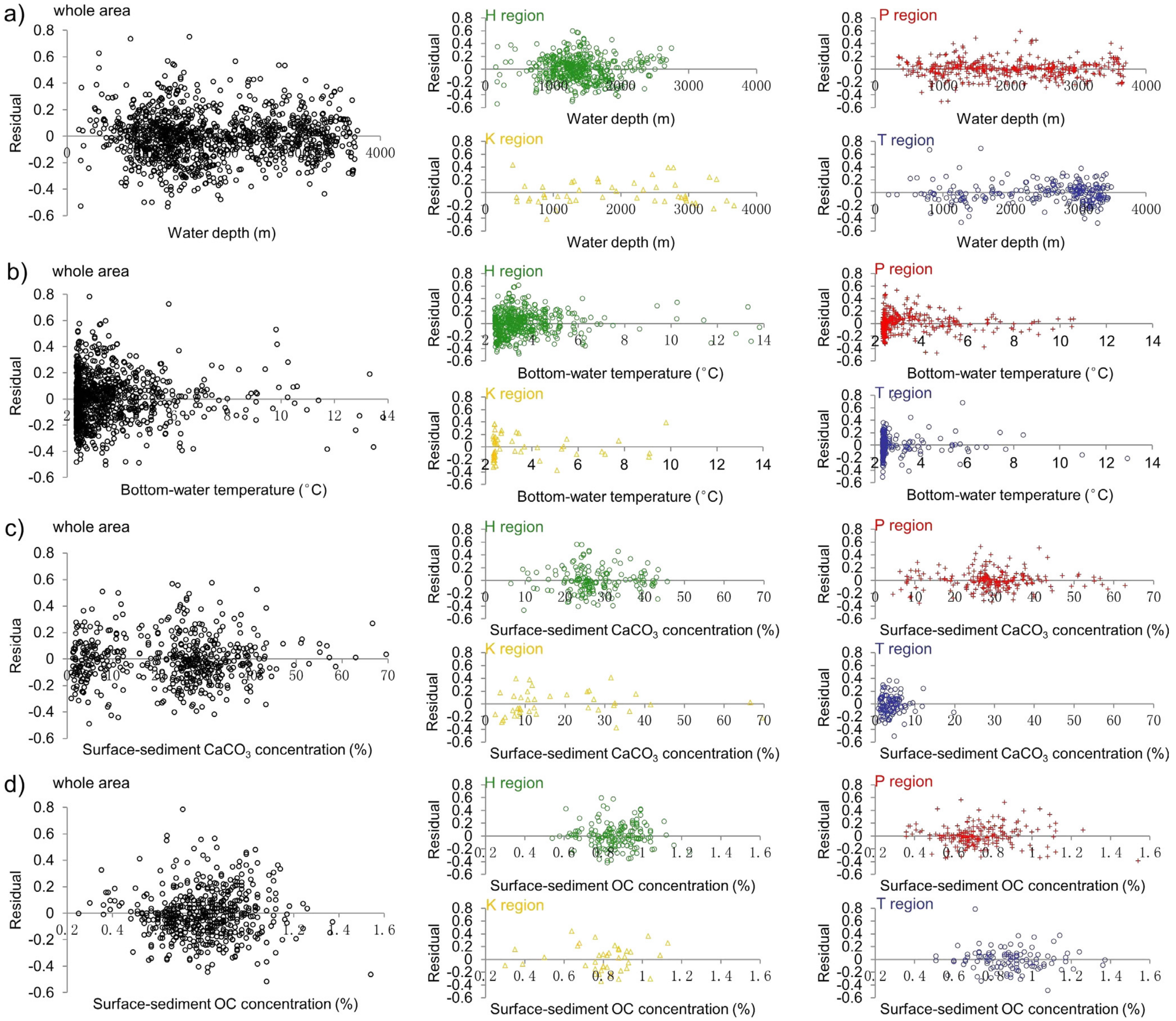

Fig. 6. Residuals of the linear regression lines in Fig. 5, between surface-sediment porewater pH and (a) water depth, (b) bottom-water temperature, (c) surface-sediment $CaCO_3$ concentration, and (d) surface-sediment OC concentration.

electrode and the test electrode together in the sediment. Previous studies have shown that pH profiles measured with such a commercial pH electrode agreed with those measured in sediment with a pH microelectrode ⩾2 cm below the sediment-water interface (Cai et al., 2006). Even if immersing a combined pH-measuring glass electrode in a suspension of charged particles can create a liquid-junction potential (Jenny et al., 1950), this “suspension effect” or “colloid effect” is negligible when measuring pH with a combined glass electrode in marine sediments (Cai, 1992; Cai and Reimers, 1993).

In the present study, we were interested in horizontal variations in the distribution of pH over the whole northern SCS, and thus used contour lines with differences of 0.2 pH unit to determine the horizontal pH gradients (Fig. 4). This led to the identification of low-pH areas with pH < 7.3 (northern part of region H, submarine canyon of region P, and region T), and the high-pH region K where pH > 7.5. Hence, small uncertainties on the in situ pH values, if present, would affect only slightly the results of our large-scale analyses and would not affect our oceanographic conclusions.

4.2. pH variations among oceanographic regions

There were large horizontal variations in pH in the northern SCS (Figs. 3 and 4), consistent with the large spatial variability exhibited by ocean-wide values of porewater pH, including the IODP data set (IODP-USIO, 2014) (Table 1). The spatial variations in porewater pH in the northern SCS could be related to differences in water-column characteristics that included upwelling, freshwater river influx, seasonal changes in circulation and KIC caused by monsoons, and geomorphical features (Fig. 8). The three areas with the lowest porewater pH were south of Hainan Island, in a submarine canyon connected to the Pearl River plume, and southwest of Taiwan Island (Figs. 3 and 4). Previous studies in northern SCS have shown that characteristics of the water column determined the sources, transport and deposition of surface sediments (Liu et al., 2013), and the accumulation of particulate organic carbon (POC) in sediments (Zhang et al., 2014). It was also shown at deep-water sites (>2000 m) in the Atlantic and the Pacific Oceans that the magnitude of the POC flux from the overlying water column was among the most important factors that determined

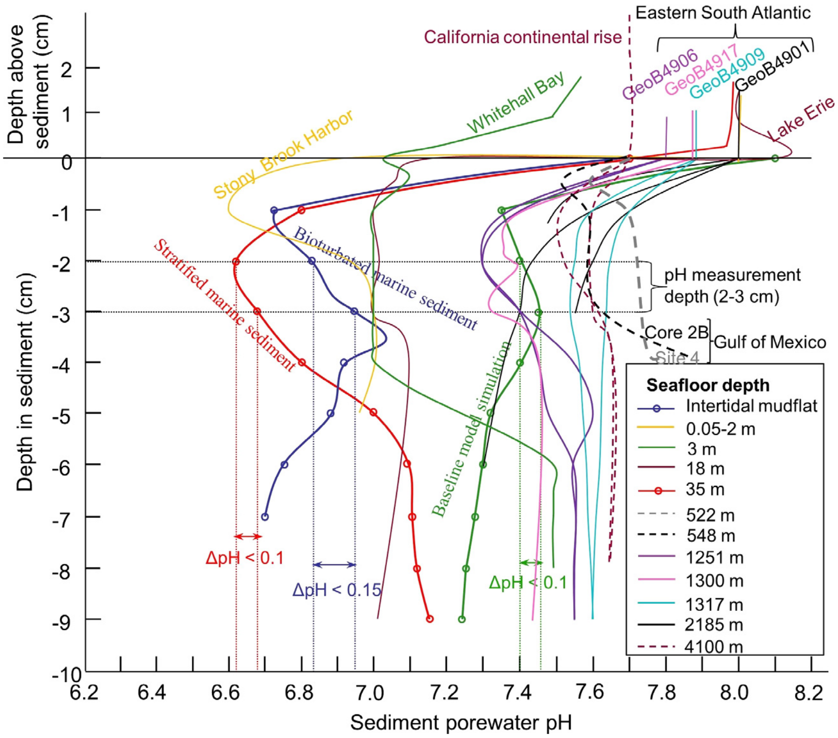

Fig. 7. Vertical profiles of pH in the upper 10 cm of surface-sediment porewater and the first 1–2 cm of the overlying water. The laboratory results (blue and red curves) were redrawn from Zhu et al. (2006), and the simulation results from a baseline model (green curve) were redrawn from Jourabchi et al. (2005). The in situ pH values for Stony Brook Harbor, Whitehall Bay, Lake Erie, the Eastern South Atlantic (GeoB4901, GeoB4906, GeoB4909, GeoB4917), the California continental rise and the Gulf of Mexico (Core 2B, Site 4) were redrawn from Fisher and Matisoff (1981), Wenzhöfer et al. (2001), Cai et al. (1995) and Cai et al. (2006), respectively. The depth interval between 2 and 3 cm corresponds to the depths of pH measurements in the present study.

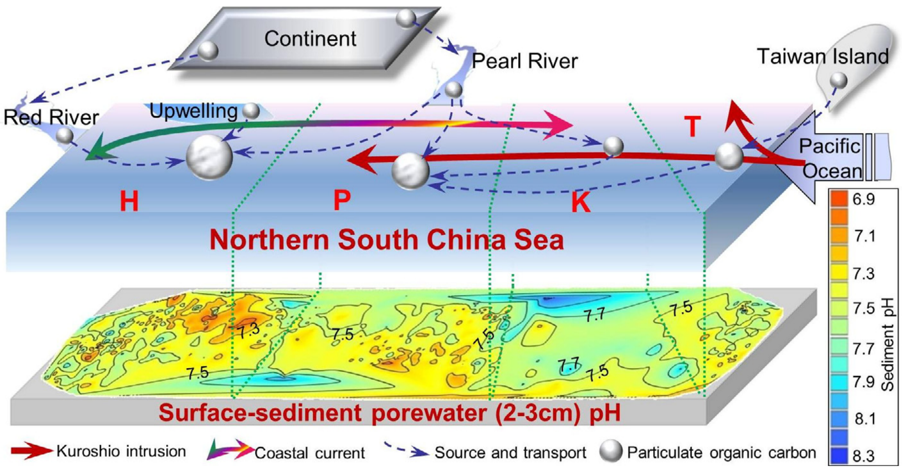

Fig. 8. Schematic representation of relationships between the horizontal variations in surface-sediment porewater pH and water-column and geomorphological characteristics in the four oceanographic regions of the northern SCS.

porewater pH (Jourabchi et al., 2008). In our dataset, the areas with high potential for POC input from the overlying water column (i.e. northern part of region H, submarine canyon in P, and region T where POC originated from upwelling or river freshwater with high POC concentrations) had low porewater pH, likely resulting from OC decomposition. However, all regions had relatively similar surface-sediment OC percent concentration (Fig. 5d), indicating that independently from the OC flux from the overlying water column, most OC in surface sediments was oxidized locally and returned as CO_2 to the water column. Hence high OC deposition from the overlying water column would usually be accompanied by intensive redox processes (including OC remineralization) in surface sediments.

The northern part of region H, South of Hainan Island, showed the lowest porewater pH in this study (<7.3). The water column there was characterized by complex processes that included the occurrence of upwelling events in surface waters (Jing et al., 2009), and freshwater input from the Pearl and Red Rivers carried by coastal circulation (Hu et al., 2000; Ou et al., 2009; Liu et al., 2013). High concentrations of POC had been reported in the water column of region H, especially in the northeastern part (Yuan et al., 2011). The high POC concentrations may have been an effect of coastal upwelling, which occurs in the northern part of region H in summer (Jing et al., 2009) and is known to often cause increased phytoplankton production (Zhang et al., 2010; Song et al., 2012). In addition, the observed high POC concentrations in the water column may have also reflected POC inputs from the Pearl and Red Rivers given that surface sediments in the northern part of region H generally originate from the two rivers (Liu et al., 2013), whose waters have high POC concentrations (Chen et al., 2006). As explained in the previous paragraph, the oxidation of the OC deposited in sediments could have contributed to porewater acidification, i.e. low pH.

The porewater pH was high in region K, and lower in region P (Fig. 4). However, previous studies (Hu et al., 2000; Shao et al., 2007; Liu et al., 2013) have suggested that the two regions are both strongly influenced by the western branch of the KIC. This current flows along the continental slope (Hu et al., 2000; Gan et al., 2006) and transports large amounts of clay minerals from Taiwan Island, which would be the general source of those minerals in surface sediments of regions K and P (Shao et al., 2007; Liu et al., 2013). Despite this similarity in the source of clay minerals, regions K and P had different pH values and concentrations of OC and $CaCO_3$. In region K, which is located on the broad continental slope southeast of Dongsha Island (Fig. 1), seismic reflection profiles have shown that the KIC has eroded away the Holocene and most of the Pleistocene sediments (Lüdmann et al., 2001; Shao et al., 2007), resulting in extensive remobilization, decomposition before burial, and transport of OC from region K to P (Blair and Aller, 2012). This may have left little OC to be decomposed and thus acidified the sediments in region K, which would explain the observed high porewater pH (>7.5) in that region. In contrast in region P, the geomorphology is characterized by the presence a large submarine canyon that crosses the continental slope, where most of the low-pH values (<7.3) are found. The northern part of the canyon was a paleo-delta front during the last glacial period, and seismic reflection profiles have shown that most sediments in region P were characterized by terrigenous material transported from the Pearl River (Lüdmann et al., 2001; Shao et al., 2007). In addition, large amount of surface-sediment clay minerals in region P originated from the Pearl River (Liu et al., 2013), indicating that this river could have been the source of most of the OC in surface sediments. Furthermore, >60% of the new POC on the northern SCS shelves is transported to the slopes and decomposed there (Chen et al., 2006). All these sources of OC combined with the OC transported from region K by the KIC would contribute to explain the low porewater pH in the submarine canyon of region P. In other words, the low pH values in the submarine canyon of region P would be related to the high pH values in region K through the transport of OC by the KIC from K to P.

In region T as in regions H and P, surface sediments had low pH, high concentrations of OC and low concentrations of $CaCO_3$ (Fig. 5). Water characteristics there were strongly influenced by the northern branch of the KIC (Hu et al., 2000; Gan et al., 2006). The low concentrations of OC and $CaCO_3$ in KIC water (Tang et al., 1998; Chen et al., 2006) could explain the low $CaCO_3$ concentrations in region T sediments. The great depth of region T (Fig. 1) could be another explanation for the low concentration of surface-sediment $CaCO_3$, i.e. most of the $CaCO_3$ would have dissolved before reaching the deep seafloor. The high OC concentration in surface sediments of region T could be related to the erosion and transport of large amounts of POC from Taiwan Island by rivers, including the Cho-Shui, Kao-ping, Erh-Jen and Tseng-Wen Rivers (Liu et al., 2013).

A previous study has shown that the pH of porewater does not necessarily reflect directly that of the overlying waters (Herlihy and Mills, 1986), which is also shown in Fig. 7 for in situ pH values in porewater and in the overlying bottom water. Our results are consistent with those of Jourabchi et al. (2008), which indicate that some characteristics of the seawater could indirectly influence the porewater pH through exchanges of OC and $CaCO_3$ between the water column and the sediments. For example, high OC rain to the seafloor, intensive redox processes in the sediments, and low $CaCO_3$ buffer capacity could lead to low porewater pH (Fig. 5). These combined mechanisms contribute to explain the observed differences in porewater pH among the four regions of the northern SCS, where the water column had contrasting characteristics (Fig. 8).

4.3. Relationships between porewater pH and water depth, bottom-water temperature, $CaCO_3$ and OC

In northern SCS, porewater pH was linearly related to water depth and bottom-water temperature in regions H, P and T (Fig. 5a, b; $p < 0.001$). The regressions analyses indicated that higher bottom-water temperature and surface-sediment pH generally occurred in shallower waters (Figs. 2 and 5). Hydrostatic pressure and bottom-water temperature can affect porewater pH through several, complex mechanisms that include changes in the dissolution constants and buffering capacity of $CaCO_3$ (Culberson and Pytkowicz, 1968; Gieskes, 1969), oxygen content for redox processes (Nealson, 1997), and bioturbation (Trevors, 1985; Arnosti et al., 1998). Among these factors, bioturbation is considered to be the dominant mode of sediment redistribution in the upper centimeters of oceanic sediments, and because the bioturbation coefficient decreases exponentially with increasing water depth, the latter could be a key variable to predict carbon accumulation, burial and remineralization (Middelburg et al., 1997). In addition, vertical transport caused by bioturbation could exceed solute transport in the uppermost layers of marine sediments (Meile and Cappellen, 2003), thus increasing the amount of oxygen taken into sediments from the overlying waters for oxic reactions and sediment acidification.

Our data showed significant positive linear relationships ($p < 0.001$) between pH and the percent concentration of solid $CaCO_3$ in region P, i.e. porewater with low pH had low $CaCO_3$ concentration, and no significant linear relationships in the three other regions (Fig. 5c; $p > 0.05$). The positive relationship in region P is consistent with in situ pH electrode measurements (Archer et al., 1989; Cai et al., 1995; Hales and Emerson, 1996), and results from both benthic flux chamber experiments (Jahnke and Jahnke, 2004) and model simulation (Jourabchi et al., 2005) showing that oxic respiration of organic carbon can drive $CaCO_3$ dissolution and decrease the porewater pH in response to metabolically produced CO_2 (Hales, 2003). It is also consistent with a previous study (Emerson and Archer, 1990) showing that within the sediment, >40% of the dissolution of particulate $CaCO_3$ was caused by OC degradation at the $CaCO_3$ saturation horizon depth, and 15–30% by dissolution above that depth. The dissolution of $CaCO_3$ in turn buffers the sediment porewater pH, and the pH of porewater is strongly related to dissolution rate of $CaCO_3$ (Jourabchi et al., 2005).

Our data did not show significant linear relationships ($p > 0.3$) between porewater pH and the percent concentration of OC (except in upwelling region H, Fig. 5d, $p = 0.003$). The absence of significant relationships in three regions may reflect OC redox processes, which are among the most important factors that affect the pH of porewater (Hales and Emerson, 1996; Reimers et al., 1996; Jourabchi et al., 2005), and depend on the magnitude of the OC input fluxes and the degradation rate of OC (Jourabchi et al., 2008). Redox processes in the water column and the sediment are responsible for the return of >99.5% of the OC to the overlying water, and the burial of <0.5% in marine sediments on the geological timescale (Burdige, 2007). Hence the lack of linear relationships between porewater pH and the percent concentration of OC in our data (except in region H, Fig. 5d) was likely because the observed OC concentrations in the surface sediments of northern SCS represented the amounts of deposited OC, and not those of oxidized OC that could have taken part in redox processes. Our results are also consistent with observations that the seafloor rates of oxic respiraton of organic carbon were relatively independent of depth and location in the offshore tropical Pacific and Atlantic, and the subtropical North Atlantic, with the exception of sediments beneath the Pacific eastern equatorial upwelling zone (Hales, 2003).

As global warming progresses, the warmer surface waters will progressively reach increasingly greater depths in some areas, and influence the sediments there. In our data, shallower and higher-temperature sediments generally had higher pH (Fig. 5a, b). In sediments, most of the OC is oxidized in the upper few centimeters, primarily utilizing dissolved molecular oxygen (Emerson and Bender, 1981; Reimers et al., 1996). In regions with shallower depths, waters affected by global warming would carry lower oxygen concentrations (i.e. gas solubility is an inverse function of water temperature), which could limit the intensive respiration of organic matter in surface sediments, leading to high porewater pH (Jourabchi et al., 2005). In addition, the higher water temperature could enhance the diffusion coefficients of ions (Li and Sandra, 1974), with the result that more H^+ could diffuse out of surface sediments into the water column, and more buffering carbonate ions could diffuse from the water column into the surface sediments. All these mechanisms could increase the pH of porewater as global warming progresses. Simultaneously the decreasing OC respiration in surface sediment and lower $CaCO_3$ solubility in both porewater and the overlying column would limit the dissolution of particulate $CaCO_3$ (Mucci, 1983; Hales, 2003) which could lead to more particulate $CaCO_3$ preserved in surface sediments.

5. Conclusions

In this study, we identified large-scale spatial pH variations in porewater (2–3 cm below the sediment surface) in the northern SCS, which could be related to characteristics of the overlying water column (Fig. 8). The relationship between porewater pH and water-column characteristics suggests that ocean acidification and global warming may have major effects on future deep-sea sediments through changes in physical and chemical characteristics of the overlying water column and exchanges at the sediment-water interface, as changes in surface-ocean temperature and pH progressively reach deeper waters.

Acknowledgements

The research cruises were organized by the Guangzhou Marine Geological Survey, China Geological Survey (http://www.hydz.cn/; shaochanggao@126.com). This work received funding from National Natural Science Foundation of China (Key Project 41430968) and the Collaborative Innovation Center for 21st-Century Maritime Silk Road Studies (2015HS05) awarded to DLT, and the Natural Gas Hydrates Major Project (GZH201100312; DD20160227), the Marine Protection Project (GZH201200512), the National High Technology Research and Development Program of China (863 Program, 2013AA092501; 2013AA0925010401), and the cooperation agreement between the Chinese Academy of Sciences and the French Centre National de la Recherche Scientifique (DLT and LL). We thank Wei-Jun Cai, College of Earth, Ocean, & Environment, University of Delaware, USA, Felice Tiu, department of Mathematics, Seattle Colleges, USA, and J.-P. Gattuso and N. Vigier, Villefranche Oceanography Laboratory, France, and anonymous reviewers for their useful comments and suggestions.

References

Archer, D., Emerson, S., Reimers, C., 1989. Dissolution of calcite in deep-sea sediments: pH and O_2 microelectrode results. Geochim. Cosmochim. Acta 53 (11), 2831–2845. http://dx.doi.org/10.1016/0016-7037(89)90161-0.

Arnosti, C., Jørgensen, B.B., Sagemann, J., Thamdrup, B., 1998. Temperature dependence of microbial degradation of organic matter in marine sediments: polysaccharide hydrolysis, oxygen consumption, and sulfate reduction. Mar. Ecol. Prog. Ser. 165, 59–70. http://dx.doi.org/10.3354/meps165059.

Ben-Yaakov, S., 1970. A method for calculating the in situ pH of seawater. Limnol. Oceanogr. 15 (2), 326–328.

Ben-Yaakov, S., 1973. PH buffering of pore water of recent anoxic marine sediments. Limnol. Oceanogr. 18 (1), 86–94. http://dx.doi.org/10.4319/lo.1973.18.1.0086.

Blair, N.E., Aller, R.C., 2012. The fate of terrestrial organic carbon in the marine environment. Ann. Rev. Mar. Sci. 4 (1), 401–423. http://dx.doi.org/10.1146/annurev-marine-120709-142717.

Blake, R.C., Shute, E.A., Greenwood, M.M., Spencer, G.H., Ingledew, W.J., 1993. Enzymes of aerobic respiration on iron. FEMS Microbiol. Rev. 11 (1–3), 9–18. http://dx.doi.org/10.1111/j.1574-6976.1993.tb00261.x.

Burdige, D.J., 2007. Preservation of organic matter in marine sediments: controls, mechanisms, and an imbalance in sediment organic carbon budgets? Chem. Rev. 107 (2), 467–485. http://dx.doi.org/10.1021/cr050347q.

Cai, W.-J., 1992. In situ Microelectrode Studies of the Hemipelagic Sediments of the Northeast Pacific Ocean (Vol Ph.D thesis). Univ. California, San Diego.

Cai, W.-J., Chen, F., Powell, E.N., Walker, S.E., Parsons-Hubbard, K.M., Staff, G.M., Wang, Y., Ashton-Alcox, K.A., Callender, W.R., Brett, C.E., 2006. Preferential dissolution of carbonate shells driven by petroleum seep activity in the Gulf of Mexico. Earth Planet. Sci. Lett. 248 (1–2), 227–243. http://dx.doi.org/10.1016/j.epsl.2006.05.020.

Cai, W.-J., Reimers, C.E., 1993. The development of pH and pCO_2 microelectrodes for studying the carbonate chemistry of pore waters near the sediment-water interface. Limnol. Oceanogr. (38) http://dx.doi.org/10.4319/lo.1993.38.8.1762.

Cai, W.-J., Reimers, C.E., Shaw, T., 1995. Microelectrode studies of organic carbon degradation and calcite dissolution at a California Continental rise site. Geochim. Cosmochim. Acta 59 (3), 497–511. http://dx.doi.org/10.1016/0016-7037(95)00316-R.

Caldeira, K., Wickett, M.E., 2003. Oceanography: anthropogenic carbon and ocean pH. Nature 425 (6956). 365–365.

Chen, C.-T.A., Wang, S.-L., Chou, W.-C., Sheu, D.D., 2006. Carbonate chemistry and projected future changes in pH and $CaCO_3$ saturation state of the South China Sea. Mar. Chem. 101 (3–4), 277–305. http://dx.doi.org/10.1016/j.marchem.2006.01.007.

Chou, W.-C., Sheu, D.D., Chen, C.T.A., Wen, L.-S., Yang, Y., Wei, C.-L., 2007. Transport of the South China Sea subsurface water outflow and its influence on carbon chemistry of Kuroshio waters off southeastern Taiwan. J. Geophys. Res. Oceans 112 (C12), C12008. http://dx.doi.org/10.1029/2007JC004087.

Culberson, C., Pytkowicz, R.M., 1968. Effect of pressure on carbonic acid, boric acid, and the pH in seawater. Limnol. Oceanogr. 13 (3), 403–417.

Dolgaleva, I.V., Gorichev, I.G., Izotov, A.D., Stepanov, V.M., 2005. Modeling of the effect of pH on the calcite dissolution kinetics. Theor. Found. Chem. Eng. 39 (6), 614–621. http://dx.doi.org/10.1007/s11236-005-0125-1.

Doney, S.C., Balch, W.M., Fabry, V.J., Feely, R.A., 2009. Ocean acidification: a critical emerging problem for the ocean sciences. Oceanography 22 (4), 16–25.

Emerson, S.R., Archer, D., 1990. Calcium carbonate preservation in the ocean. Philos. Trans. Roy. Soc. Lond. Ser. A Math. Phys. Sci. 331 (1616), 29–40.

Emerson, S.R., Bender, M., 1981. Carbon fluxes at the sediment-water interface of the deep-sea: calcium carbonate preservation. J. Mar. Res. 39 (1), 139–162.

Expedition 302 Scientists, 2006. Methods. In: Backman, J., Moran, K., McInroy, D.B., Mayer, L.A., Scientists, E. (Eds.), Proceedings of the Integrated Ocean Drilling Program, vol. 302. Integrated Ocean Drilling Program Management International Inc, Tokyo.

Expedition 329 Scientists, 2011. Methods. In: D'Hondt, S., Inagaki, F., Alvarez Zarikian, C.A., Scientists, E. (Eds.), Proceedings of the Integrated Ocean Drilling Program, vol. 329. Integrated Ocean Drilling Program Management International Inc., Tokyo.

Fisher, J.B., Matisoff, G., 1981. High resolution vertical profiles of pH in recent sediments. Hydrobiologia 79 (3), 277–284. http://dx.doi.org/10.1007/BF00006325.

Franz, A., 1991. Voronoi diagrams – a survey of a fundamental geometric data structure. ACM Comput. Surv. 23 (3), 345–405.

Gan, J., Li, H., Curchitser, E.N., Haidvogel, D.B., 2006. Modeling South China Sea circulation: response to seasonal forcing regimes. J. Geophys. Res. Oceans 111 (C6), C06034. http://dx.doi.org/10.1029/2005JC003298.

Gattuso, J.-P., Epitalon, J.-M., Lavigne, H., Orr, J., Gentili, B., Hofmann, A., Proye, A., Soetaert, K., Rae, J., 2014. Seacarb: Seawater Carbonate Chemistry with R. R Package Version 3.0.3.

Gieskes, J.M., 1969. Effect of temperature on the pH of seawater. Limnol. Oceanogr. 14 (5), 679–685.

Hales, B., 2003. Respiration, dissolution, and the lysocline. Paleoceanography 18 (4), 1099. http://dx.doi.org/10.1029/2003PA000915.

Hales, B., Emerson, S., 1996. Calcite dissolution in sediments of the Ontong-Java Plateau: in situ measurements of pore water O_2 and pH. Global Biogeochem. Cycles 10 (3), 527–541. http://dx.doi.org/10.1029/96GB01522.

Hales, B., Emerson, S., 1997. Calcite dissolution in sediments of the Ceara Rise: in situ measurements of porewater O_2, pH, and CO_2(aq). Geochim. Cosmochim. Acta 61 (3), 501–514. http://dx.doi.org/10.1016/S0016-7037(96)00366-3.

Hales, B., Emerson, S., Archer, D., 1994. Respiration and dissolution in the sediments of the western North Atlantic: estimates from models of in situ microelectrode measurements of porewater oxygen and pH. Deep Sea Res. Part I 41 (4), 695–719. http://dx.doi.org/10.1016/0967-0637(94)90050-7.

Herlihy, A.T., Mills, A.L., 1986. The pH regime of sediments underlying acidified waters. Biogeochemistry 2 (1), 95–99. http://dx.doi.org/10.1007/BF02186967.

Houghton, J.T., Ding, Y., Griggs, D.J., Noguer, M., Van der Linden, P.J., Dai, X., Maskell, K., Johnson, C.A., 2001. Climate change 2001: The scientific basis. In: Contribution of Working Group I to the Third Assessment Report of the Intergovernmental Panel on Climate Change. Cambridge University Press, Cambridge, United Kingdom and New York, NY, USA.

Hu, J., Kawamura, H., Hong, H., Qi, Y., 2000. A review on the currents in the south china sea: seasonal circulation, south china sea warm current and Kuroshio intrusion. J. Oceanogr. 56 (6), 607–624. http://dx.doi.org/10.1023/A:1011117531252.

Hunter, K.A., 1998. The temperature dependence of pH in surface seawater. Deep Sea Res. Part I 45 (11), 1919–1930. http://dx.doi.org/10.1016/S0967-0637(98)00047-8.

IODP-USIO, 2014. Core Database. U.S. Implementing Organization (IODP-USIO). <http://iodp.tamu.edu/database/>.

Jahnke, R.A., Jahnke, D.B., 2004. Calcium carbonate dissolution in deep sea sediments: reconciling microelectrode, pore water and benthic flux chamber results. Geochim. Cosmochim. Acta 68 (1), 47–59. http://dx.doi.org/10.1016/S0016-7037(03)00260-6.

Jenny, H., Nielsen, T.R., Coleman, N.T., Williams, D.E., 1950. Concerning the measurement of pH, ion activities, and membrane potentials in colloidal systems. Science 112 (2902), 164–167. http://dx.doi.org/10.1126/science.112.2902.164.

Jing, Z.-Y., Qi, Y.-Q., Hua, Z.-L., Zhang, H., 2009. Numerical study on the summer upwelling system in the northern continental shelf of the South China Sea. Cont. Shelf Res. 29 (2), 467–478. http://dx.doi.org/10.1016/j.csr.2008.11.008.

Jourabchi, P., Meile, C., Pasion, L.R., Van Cappellen, P., 2008. Quantitative interpretation of pore water O_2 and pH distributions in deep-sea sediments. Geochim. Cosmochim. Acta 72 (5), 1350–1364. http://dx.doi.org/10.1016/j.gca.2007.12.012.

Jourabchi, P., Van Cappellen, P., Regnier, P., 2005. Quantitative interpretation of pH distributions in aquatic sediments: a reaction-transport modeling approach. Am. J. Sci. 305 (9), 919–956. http://dx.doi.org/10.2475/ajs.305.9.919.

Lüdmann, T., Kin Wong, H., Wang, P., 2001. Plio-quaternary sedimentation processes and neotectonics of the northern continental margin of the South China Sea. Mar. Geol. 172 (3–4), 331–358. http://dx.doi.org/10.1016/S0025-3227(00)00129-8.

Li, Y.-H., Sandra, G., 1974. Diffusion of ions in sea water and in deep-sea sediments. Geochim. Cosmochim. Acta 38 (5), 703–714.

Liu, J., Xiang, R., Chen, Z., Chen, M., Yan, W., Zhang, L., Chen, H., 2013. Sources, transport and deposition of surface sediments from the South China Sea. Deep Sea Res. Part I 71, 92–102. http://dx.doi.org/10.1016/j.dsr.2012.09.006.

Liu, Z., Fan, H., Zhao, S., 2002. The Geology of South China Sea. Science Press, Beijing.

Luo, X., Xu, X., Zhang, Z., Chen, Z., 2007. Development and technical character of XXG-T marine geothermal gradient measurement system. Geol. Res. South China Sea 00, 102–110.

Ma, Y.A., Xu, H.Z., Yu, T., He, G.K., Zhao, Y.Y., Fu, Y.Z., 2008. The Specification for Marine Monitoring-Part 5: Sediment Analysis. China Standardization Press, Beijing.

Meile, C., Cappellen, P.V., 2003. Global estimates of enhanced solute transport in marine sediments. Limnol. Oceanogr. 48 (2), 777–786.

Middelburg, J.J., Soetaert, K., Herman, P.M.J., 1997. Empirical relationships for use in global diagenetic models. Deep Sea Res. Part I 44 (2), 327–344. http://dx.doi.org/10.1016/S0967-0637(96)00101-X.

Mucci, A., 1983. The solubility of calcite and aragonite in seawater at various salinities, temperatures, and one atmosphere total pressure. Am. J. Sci. 283 (7), 780–799. http://dx.doi.org/10.2475/ajs.283.7.780.

Murray, J.W., Emerson, S., Jahnke, R., 1980. Carbonate saturation and the effect of pressure on the alkalinity of interstitial waters from the Guatemala Basin. Geochim. Cosmochim. Acta 44 (7), 963–972. http://dx.doi.org/10.1016/0016-7037(80)90285-9.

Nealson, K.H., 1997. Sediment bacteria: who's there, what are they doing, and what's new? Annu. Rev. Earth Planet. Sci. 25, 403–434. http://dx.doi.org/10.1146/annurev.earth.25.1.403.

Ou, S., Zhang, H., Wang, D.-X., 2009. Dynamics of the buoyant plume off the Pearl River Estuary in summer. Environ. Fluid Mech. 9 (5), 471–492. http://dx.doi.org/10.1007/s10652-009-9146-3.

Reimers, C.E., Ruttenberg, K.C., Canfield, D.E., Christiansen, M.B., Martin, J.B., 1996. Porewater pH and authigenic phases formed in the uppermost sediments of the Santa Barbara Basin. Geochim. Cosmochim. Acta 60 (21), 4037–4057.

Sabine, C.L., Feely, R.A., Gruber, N., Key, R.M., Lee, K., Bullister, J.L., Wanninkhof, R., Wong, C.S., Wallace, D.W.R., Tilbrook, B., Millero, F.J., Peng, T.-H., Kozyr, A., Ono, T., Rios, A.F., 2004. The oceanic sink for anthropogenic CO_2. Science 305 (5682), 367–371. http://dx.doi.org/10.1126/science.1097403.

Shao, L., Li, X., Geng, J., Pang, X., Lei, Y., Qiao, P., Wang, L., Wang, H., 2007. Deep water bottom current deposition in the northern South China Sea. Sci. China, Ser. D Earth Sci. 50 (7), 1060–1066. http://dx.doi.org/10.1007/s11430-007-0015-y.

Sibson, R., 1981. A brief description of natural neighbor interpolation (chapter 2). In: Barnett, V. (Ed.), Interpreting Multivariate Data. John Wiley & Sons, New York, pp. 21–36.

Song, X., Lai, Z., Ji, R., Chen, C., Zhang, J., Huang, L., Yin, J., Wang, Y., Lian, S., Zhu, X., 2012. Summertime primary production in northwest South China Sea: interaction of coastal eddy, upwelling and biological processes. Cont. Shelf Res. 48, 110–121. http://dx.doi.org/10.1016/j.csr.2012.07.016.

Sun, Q., Tang, D., Wang, S., 2012. Remote-sensing observations relevant to ocean acidification. Int. J. Remote Sens. 33 (23), 7542–7558. http://dx.doi.org/10.1080/01431161.2012.685978.

Tang, D., Kawamura, H., Doan-Nhu, H., Takahashi, W., 2004. Remote sensing oceanography of a harmful algal bloom off the coast of southeastern Vietnam. J. Geophys. Res. Oceans 109 (C3), C03014. http://dx.doi.org/10.1029/2003JC002045.

Tang, D., Kester, D.R., Ni, I.H., Kawamura, H., Hong, H., 2002. Upwelling in the Taiwan Strait during the summer monsoon detected by satellite and shipboard measurements. Remote Sens. Environ. 83 (3), 457–471. http://dx.doi.org/10.1016/S0034-4257(02)00062-7.

Tang, D., Ni, I.H., Müller-Karger, F.E., Liu, Z.J., 1998. Analysis of annual and spatial patterns of CZCS-derived pigment concentration on the continental shelf of China. Cont. Shelf Res. 18 (12), 1493–1515. http://dx.doi.org/10.1016/S0278-4343(98)00039-9.

Trevors, J.T., 1985. Effect of temperature on selected microbial activities in aerobic and anaerobically incubated sediment. Hydrobiologia 126 (2), 189–192. http://dx.doi.org/10.1007/BF00008686.

Wang, S.M., Yan, W.H., Zheng, C.J., Dong, G.X., 2010. Method for Chemical Analysis of Rocks and Ores-General Rulers and Regulations. China Standardization Press, Beijing.

Wenzhöfer, F., Adler, M., Kohls, O., Hensen, C., Strotmann, B., Boehme, S., Schulz, H. D., 2001. Calcite dissolution driven by benthic mineralization in the deep-sea: in situ measurements of Ca^{2+}, pH, pCO_2 and O_2. Geochim. Cosmochim. Acta 65 (16), 2677–2690. http://dx.doi.org/10.1016/S0016-7037(01)00620-2.

Wolaver, T.G., Zieman, J., Kjerfve, B., 1986. Factors affecting short-term variability in sediment pH as a function of marsh elevation in a Virginia mesohaline marsh. J. Exp. Mar. Biol. Ecol. 101, 227–237.

Yan, M.H., Huang, H.P., 1993. Method for Chemical Analysis of Rocks and Ores-General Rules and Regulations. China Standardization Press, Beijing.

Yanagawa, K., Morono, Y., de Beer, D., Haeckel, M., Sunamura, M., Futagami, T., Hoshino, T., Terada, T., Nakamura, K.-I., Urabe, T., Rehder, G., Boetius, A., Inagaki, F., 2013. Metabolically active microbial communities in marine sediment under high-CO_2 and low-pH extremes. ISME J. 7 (3), 555–567 <http://www.nature.com/ismej/journal/v7/n3/suppinfo/ismej2012124s1.html>.

Yuan, X., He, L., Yin, K., Pan, G., Harrison, P.J., 2011. Bacterial distribution and nutrient limitation in relation to different water masses in the coastal and northwestern South China Sea in late summer. Cont. Shelf Res. 31 (11), 1214–1223. http://dx.doi.org/10.1016/j.csr.2011.04.012.

Zhang, W.Y., Zhang, C.M., Xu, K.C., Wang, H.C., Chen, B.L., Gu, G.L., 1998. The Specification for Marine Monitoring-Part 5: Sediment Analysis. China Standardization Press, Beijing.

Zhang, Y., Dong, J., Ling, J., Wang, Y., Zhang, S., 2010. Phytoplankton distribution and their relationship to environmental variables in Sanya Bay, South China Sea. Sci. Mar. 74 (4), 783–792.

Zhang, Y., Kaiser, K., Li, L., Zhang, D., Ran, Y., Benner, R., 2014. Sources, distributions, and early diagenesis of sedimentary organic matter in the Pearl River region of the South China Sea. Mar. Chem. 158, 39–48. http://dx.doi.org/10.1016/j.marchem.2013.11.003.

Zhu, Q., Aller, R.C., Fan, Y., 2006. Two-dimensional pH distributions and dynamics in bioturbated marine sediments. Geochim. Cosmochim. Acta 70 (19), 4933–4949. http://dx.doi.org/10.1016/j.gca.2006.07.033.